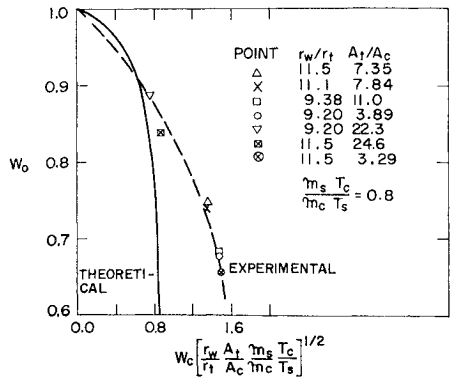

Fig. 5 Comparison of the experimental vortex valve data with theoretical predictions.

system was used. Helium at room temperature was chosen for the control gas because its ratio of T/M closely approximates T_s/M_s. The control mass flow was measured by means of an upstream sonic orifice.

The end-burning propellant[6] was a 15% aluminum, 70% ammonium perchlorate composition with carboxyl-terminated polybutadiene binder, with $n \approx 0.42$, $\dot{r} \approx 0.21$ in./sec at 300 psia, $T_s \approx 5000°$R, and $M_s \approx 30$. Graphite nozzle inserts and a pyrolytic graphite VV supply flow diaphragm were required to withstand the erosive effects of the aluminized propellant. The flow diaphragm held up remarkably well and showed less than $\frac{1}{8}$ in. stagnation-point erosion after more than 100 sec of operation. The combustion products contained almost 30% liquid Al_2O_3, much of which condensed on the internal surfaces of the motor and valve. With the valve attached to the motor, it was found that the deposited material represented 15% of the total propellant mass. This mass sink effect proved to be the greatest source of experimental uncertainty.

The control flow was cycled on and off during each run producing similar step responses in P_s (Fig. 4). The test results (normalized in terms of W_0, W_c and the scaling factor) in Fig. 5 show that performance fell short of theoretical as control flow was increased. This was not unexpected as performance may be degraded by boundary-layer effects, control flow mixing and ducting losses, heat transfer, mass sink effect, and swirl destruction causes by material deposited within the valve chamber.

Figure 6 contains the experimental data of pressure ratio vs η, and compares it with the performance that could be expected from straight mass augmentation. The error bars represent the uncertainty in total mass flow due to the mass sink effect.[6] In spite of the low burning rate exponent, the valve produced an effect over 230% greater than would be predicted for straight mass augmentation. A maximum experimental pressure ratio of 5.45 was obtained.

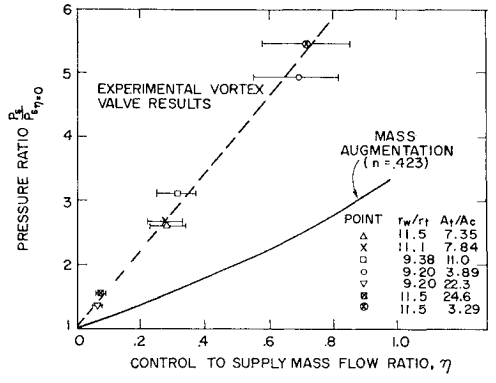

Fig. 6 Solid-propellant chamber pressure as a function of secondary flow.

Concluding Remarks

It is shown in Fig. 6 that the VV yields far better performance than mass augmentation giving the $VVRM$ greater flexibility for the same expenditure of control flow. This superiority would be even more impressive with a more efficient valve and a higher burning rate exponent (see Fig. 2). Increased stability and continuous throttling are inherent advantages of the vortex valve.

The successful performance of the pyrolytic graphite flow diaphragm is a positive indication that plates of high-temperature materials can be mounted directly in the main propellant exhaust stream. Lightweight composites (e.g., graphite, oxides, ablatives) are necessary to ensure structural integrity and minimize the condensation of exhaust products on surfaces that otherwise would have to be cooled.

Concepts such as staged series vortex valves and bidirectional control flow injection may yield further increases in system flexibility and performance.

References

[1] Nelson, C., Roberts, R., and Fish, V., "The Vortex Valve Controlled Rocket Motor," AIAA Paper 68-538, Atlantic City, N.J., 1968.

[2] Blatter, A. and Keranen, T. W., "A Vortex Valve for Flow Modulation of 5500°F Gas," *Journal of Spacecraft and Rockets*, Vol. 7, No. 2, Feb. 1970, pp. 169–174.

[3] Bauer, A. B., "Vortex Valve Operation in a Vacuum Environment," ASME Paper 68-FE-47, Philadelphia, Pa., May 1968.

[4] Lewellen, W. S., Burns, W. J., and Strickland, H. J., "Transonic Swirling Flow," *AIAA Journal*, Vol. 7, No. 7, July 1969, pp. 1290–1297.

[5] Glick, R. L. and Kilgore, M. S., "Effect of Specific Heat Ratio on Mass Flow for Swirling Nozzle Flow," *Journal of Spacecraft and Rockets*, Vol. 4, No. 8, Aug., 1967, p. 1098.

[6] Walsh, R. F., "Investigation of a Solid Propellant Rocket Motor Modulated by a Fluidic Vortex Valve," S.M. thesis, Sept. 1969, M.I.T., Cambridge, Mass.

Iterative Solution of a Radiation Dominated Heat Balance

CHARLES W. BOLZ JR.*
Rocket Research Corporation, Redmond, Wash.

Nomenclature

T_i = temperature of node i
R_{ij} = thermal resistance between nodes i and j
σ = Stefan-Boltzmann constant
$\bar{A}\bar{F}_{ij}$ = radiation interchange factor between nodes i and j
q_i = heat generation at node i
β = over-relaxation factor

Introduction

MODERN spacecraft thermal design makes extensive use of concepts such as heat shielding and multilayer insulation (superinsulation) which exploit the fourth-power temperature dependence of radiation heat transfer. However, the analytical model representing the thermal design is normally solved by numerical techniques developed for linear equations.[1] Certain of these techniques are iterative and may be extended to handle radiation heat transfer by use of a temperature-dependent radiation coefficient (radiation resistance) which is recomputed at each iteration.[2,3] This

Received October 9, 1970.
* Associate Analysis Engineer. Member AIAA.

approach is quite satisfactory as long as the radiative coefficients about each node are of similar magnitude to the conductive coefficients. Instability arises, however, about heat shield or superinsulation nodes where the radiative terms dominate.[3] This Note presents a stable method for solving the heat balance about such nodes.

Development

About any node i an equilibrium energy balance may be written as follows:

$$\Sigma_j[(T_j - T_i)/R_{ij}] + \Sigma_j\sigma\bar{A}\bar{F}_{ij}(T_j^4 - T_i^4) + q_i = 0 \quad (1)$$

When the radiation term is absent, Eq. (1) is typically rearranged and solved for T_i by means of some over-relaxation technique.

$$T_i = (1 - \beta)T_i + \beta\left[\frac{\Sigma_j(T_j/R_{ij}) + q_i}{\Sigma_j(1/R_{ij})}\right] \quad (2)$$

This approach is extended to radiation by defining a radiation resistance equal to the temperature potential divided by the radiative heat flux at the previous iteration:

$$R(\text{rad}) = 1/\sigma\bar{A}\bar{F}_{ij}(T_i^2 + T_j^2)(T_i + T_j) \quad (3)$$

For radiation dominated heat balances, however, it is useful to solve Eq. (1) for the T_i appearing in the radiative term. This yields the expression:

$$T_i = \left[\frac{\Sigma_j\sigma\bar{A}\bar{F}_{ij}T_j^4 + \Sigma_j[(T_j - T_i)/R_{ij}] + q_i}{\Sigma_j\sigma\bar{A}\bar{F}_{ij}}\right]^{1/4} \quad (4)$$

which may be used wherever Eq. (2) is unstable.

Discussion

Equation (4) has been extensively tested using the Rocket Research Corporation Thermal Analyzer Program.[4] The analyst specifies those nodes for which Eq. (4) is to be used; Eq. (2) is then used for all other nodes. Equation (4) has converged quickly in all cases to date for which Eq. (2) was unsatisfactory. Equation (4) is also used for transient solutions when the node thermal mass is negligible and the implicit assumption of thermal equilibrium with the connecting nodes is tenable.

References

[1] Forsythe, G. E. and Wasow, W. R., "Finite Difference Methods for Partial Differential Equations," Wiley, New York, 1960, Ch. 3.

[2] Schultz, H. D., "Thermal Analyzer Program for the Solution of General Heat Transfer Problems," LR 18902, Ch. 4, 1965, Lockheed California Company, Sunnyvale, Calif.

[3] "Boeing Thermal Analyzer Engineering Usage Guide," AS0315, 1962, The Boeing Company, Seattle, Wash., pp. 18, 28.

[4] Bolz, C. W., "Rocket Research Corporation Thermoanalyzer Program User's Manual," RRC 68-ES-57R1, March 1969, Rocket Research Corporation, Seattle, Wash.